Measurement of the Mueller matrix for ocean water

Kenneth J. Voss and Edward S. Fry

The normalized light scattering polarization matrix has been measured for ocean water using an electrooptic light scattering polarimeter. Measurements were done on samples from the Atlantic and Pacific Oceans and the Gulf of Mexico. The polarization effects in the matrices were found to have, in general, a form which is similar to polarization effects in the Rayleigh scattering approximation; for example, all off-diagonal matrix elements except S12 and S21 were zero. Mueller matrix elements were calculated using a Mie computer code and compared to the measured matrices for ocean water. A simple one-component distribution was found to produce a reasonably good fit.

I. Introduction

Light scattering has been used extensively in oceanography to obtain information on the properties of ocean water and particulates in the ocean. Physical oceanographers use light scattering and light attenuation to investigate suspended sediments.[1] Biological oceanographers use light scattering to determine both the biological content of the water and the physiological state of plankton in the water.[2,3] In remote sensing, scattered light is used to determine properties of the particulates in the seawater and must also be taken into account when measuring other oceanographic parameters.[4]

Although many measurements of light scattering in seawater have been made, the majority of these measurements have observed only the intensity of the scattered light. To gain all the information that is available in elastic light scattering, one must observe changes in the polarization of the light. The polarization effects provide important data which may help in characterizing both physical and physiological states of particulates in ocean water.

Previous measurements of the Mueller matrix of ocean water have been disparate. The first measurements, done by Beardsley,[5] were on samples from four locations: Boston Harbor, New England coastal water, North Atlantic Ocean, and the Charles River. It was found that the Mueller matrices for these samples were very symmetric and had the general form of the normalized Rayleigh approximation matrix.

Measurements of the Mueller matrix by Kadyshevich in the Black Sea,[6] Atlantic and Pacific Oceans,[7] and Baltic Sea[8] indicated large variations in the symmetry and magnitude of the matrix elements with sample location and depth. Many of the normalized off-diagonal elements in the Mueller matrix were as large as 40% of full scale. These measurements led one to believe that much information on the shape and symmetries of the particulates could be gained from the measurement of the Mueller matrix for ocean water.

II. Theory

To quantify changes in the polarization, one must have a way of describing the polarization of a light beam as well as the transformations that take place due to the scattering process. A convenient representation of the polarization of a light beam is the Stokes vector.[9] The four elements of this vector, labeled I, Q, U, and V, are defined in terms of the electric field as

$$\begin{aligned} \mathrm{I} &= E_\mathrm{l}^2 + E_\mathrm{r}^2, & \mathrm{U} &= 2E_\mathrm{l}E_\mathrm{r}\cos\delta, \\ \mathrm{Q} &= E_\mathrm{l}^2 - E_\mathrm{r}^2, & \mathrm{V} &= 2E_\mathrm{l}E_\mathrm{r}\sin\delta, \end{aligned} \tag{1}$$

where E_l and E_r, the components of the total electric field, and δ, the relative phase, are defined by

$$E = E_\mathrm{l}\cos(kz - \omega t + \varepsilon_\mathrm{l})\hat{l} + E_\mathrm{r}\cos(kz - \omega t + \varepsilon_\mathrm{r})\hat{r}, \tag{2}$$

$$\delta = \varepsilon_\mathrm{l} - \varepsilon_\mathrm{r},$$

where $\hat{l}$ is a unit vector parallel to the scattering plane and $\hat{r}$ is a unit vector perpendicular to the scattering plane. Qualitatively, I corresponds to the total intensity of the light beam, Q to the degree of linear polarization in the $\hat{l}$ and $\hat{r}$ directions, U to the degree of linear polarization at 45° to the $\hat{l}$ and $\hat{r}$ directions, and V is the degree of circular polarization. The principle of optical equivalence, first derived by Stokes,[10] shows that the Stokes vector is a complete representation of the polarization state of a light beam.

The authors are with Texas A&M University, Physics Department, College Station, Texas 77843.

Received 19 May 1984.
0003-6935/84/234427-13$02.00/0.

In a suspension of particulates, individual particles will be in random positions. Therefore, the light scattered from any two of the particules will not have a specific phase relationship, and the scattered light will add incoherently. In this case, the Stokes vector is the sum of the individual vectors.

When a light beam is scattered by a particle, or changed by an optical element, the Stokes vector of the light beam undergoes a linear transformation to a new Stokes vector. This transformation can be represented by a 4 × 4 matrix called the Mueller or polarization matrix. Specifically, we have

$$\begin{bmatrix} I' \\ Q' \\ U' \\ V' \end{bmatrix} = \begin{bmatrix} M11 & M12 & M13 & M14 \\ M21 & M22 & M23 & M24 \\ M31 & M32 & M33 & M34 \\ M41 & M42 & M43 & M44 \end{bmatrix} \begin{bmatrix} I \\ Q \\ U \\ V \end{bmatrix}, \quad (3)$$

where (I,Q,U,V) is the Stokes vector of the incident light and (I′,Q′,U′,V′) is the Stokes vector of the scattered or transmitted light. The Stokes vector contains all the polarization information that can be measured for a light beam, therefore, the Mueller matrix contains all the polarization information in an elastic scattering process.

As with the case of the Stokes vector, the Mueller matrix of a suspension of particulates is the sum of the Mueller matrices of the individual particles.

It is advantageous, when looking at polarization effects in the Mueller matrix, to normalize the matrix to the M11 component:

$$\begin{bmatrix} 1 & S12 & S13 & S14 \\ S21 & S22 & S23 & S24 \\ S31 & S32 & S33 & S34 \\ S41 & S42 & S43 & S44 \end{bmatrix}, \quad (4)$$

where $Sij = Mij/M11$. In this way, intensity dependent effects can be isolated from the polarization effects, both to simplify analysis and highlight the latter. The normalized matrix elements, Sij can only have values between −1 and +1. All of our measured matrices are normalized electronically in the process of measurement and are presented in normalized form. Errors are quoted in terms of this normalized full scale value of unity.

III. Experimental Procedures

Previous measurements of the Mueller matrix for ocean water were made with photometers modified by using combinations of quarterwave plates and linear polarizers to prepare the incident light beam and analyze the scattered light. By using sixteen different combinations of optical elements and algebraically manipulating the scattered intensity measurements for each combination, the Mueller matrix could be determined. Unfortunately, the differences of nearly equal quantities must be taken, resulting in a loss of significant figures. Thus, an uncertainty in measuring the intensity of the light of 5–10% (as quoted by Beardsley[5]) can result in appreciably larger errors in the normalized matrix elements. In addition, these measurements typically took over 2 h to complete, thus the sample may change physically or physiologically during the course of the measurement.

The instrument used in the present study was an electrooptic light scattering photometric polarimeter. An instrument similar to the one used here has previously been used to measure single particles and suspensions of particles and is described in detail by Thompson[11] and Thompson *et al.*[12] Basically, the instrument has two electrooptic modulators which modulate the polarization of the incident light beam through a basis set of Stokes vectors at audio frequencies. The scattered light passes through two more electrooptic modulators, a linear polarizer, and is incident on a photomultiplier tube. With these four modulators the Mueller matrix elements can be measured as the amplitudes at different audio frequencies in the photomultiplier tube signal. Approximately 2 min are required to measure the entire matrix at scattering angles from 10° to 160°. The problems involved in taking algebraic differences of measured quantities are circumvented by effectively taking analog differences at audio frequencies.

The light source used for all the data presented here was an argon-ion laser operating at a wavelength of 488 nm. Other more specific details of the present instrument are described by Voss.[13] A salient feature was the sample cell design. Specifically, the water sample was held in a 100-cm diam cylindrical Pyrex sample cell. Neutral density filters were arranged in the cell to prevent scattered light from reentering the scattering volume. These neutral density filters also prevent the direct, unscattered light beam from reflecting off the exit window of the sample cell and into the scattering volume.

Water samples were obtained from Nisken bottles filled during hydrocasts. Approximately 0.5 liters of water were required to make the measurements. Each sample was measured three times and then the data from these samples were averaged to reduce the effect of noise and of random fluctations in the sample. An aqueous suspension of 91-nm polystyrene spheres was measured before and after each set of ocean samples to check the instrument for systematic effects.

The data presented are the scattering due to both pure water and the particulates suspended in the water. However, the intensity of the scattered light due to pure water is over an order of magnitude less than that due to the clearest ocean sample measured, thus scattering effects due to pure water are completely negligible in the normalized matrix.

IV. Measurements

Over 200 matrices have been measured in the Gulf of Mexico, Pacific Ocean, and Atlantic Ocean. In the Pacific Ocean samples were taken from upwelling zones off Big Sur California, across frontal zones, and in coastal waters of Baja Mexico. In the Atlantic Ocean, measurements were taken at positions on the continental shelf, at the shelf break, the Gulf Stream, and in the Sargasso Sea. In the Gulf of Mexico, measurements

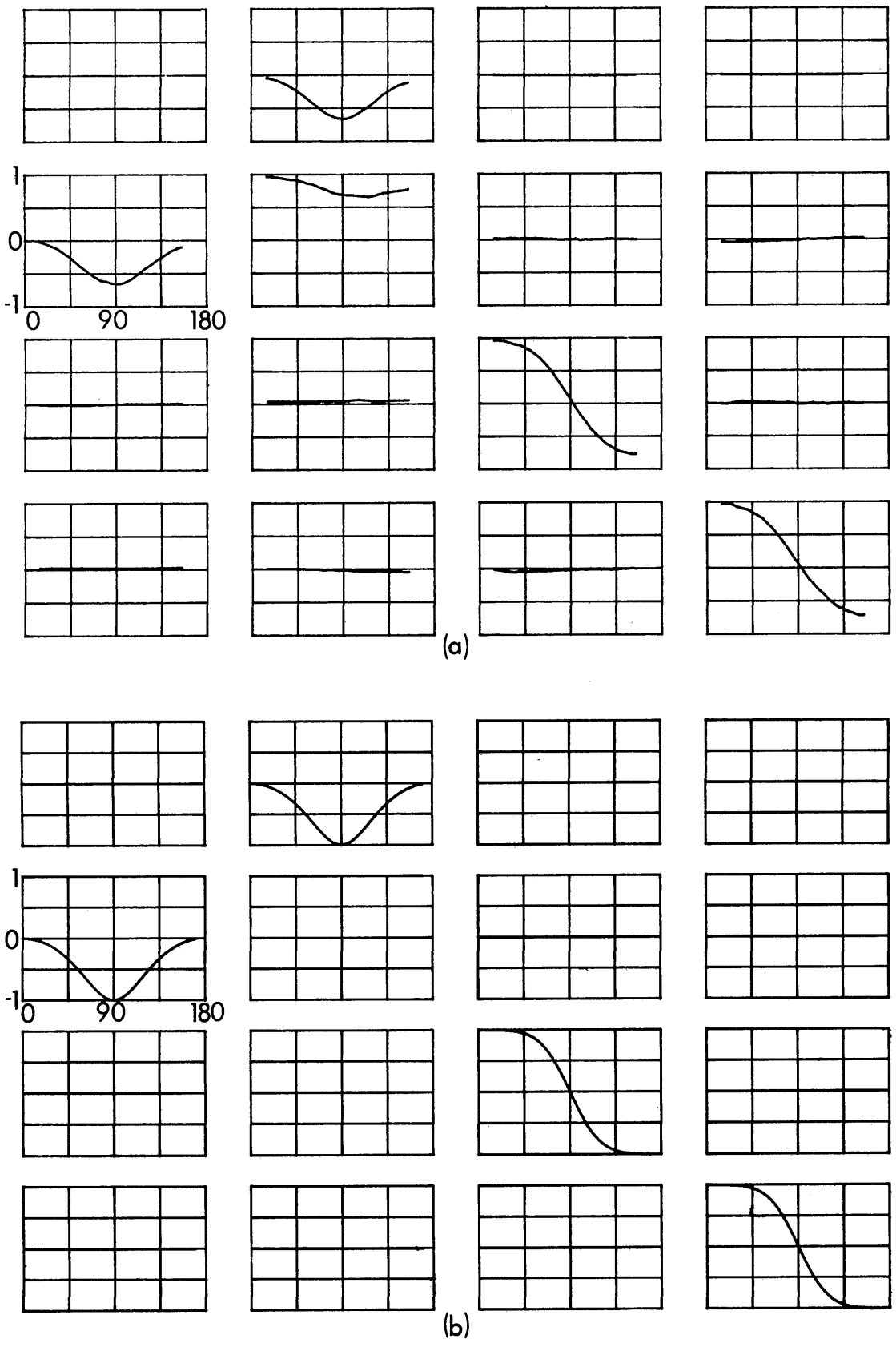

Fig. 1. (a) The average Mueller matrix of the Pacific and Atlantic Oceans. The x axis of each graph corresponds to the scattering angle, the y axis corresponds to the normalized matrix element value. (b) The calculated Mueller matrix of particles in the Rayleigh-Gans approximation.

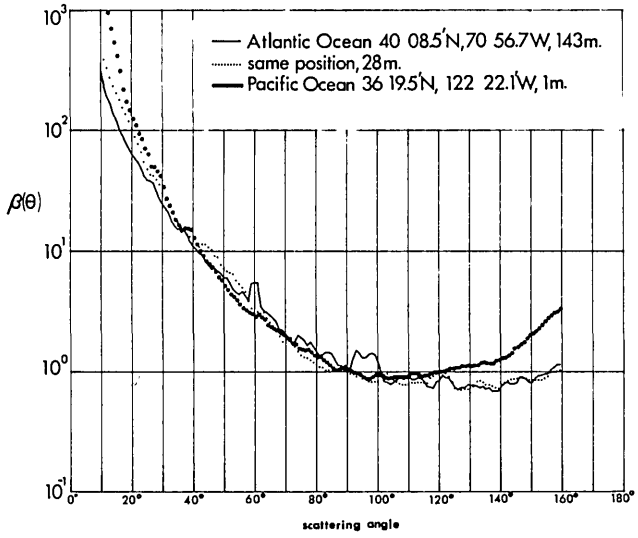

Fig. 2. Volume scattering function for three samples.

were taken at locations from the mouth of Galveston Bay to out beyond the shelf break, concentrating in the Western Gulf. The scattering at 45°, i.e., $\beta(45)$, taken by some investigators to be correlated to the total scattering coefficient b,[14] varied by more than an order of magnitude in the ensemble of samples. In all but one of these measurements the matrices were similar to those shown in Fig. 1(a). The exception differed only in that it showed a real effect at the 10% level in S34 and S43. It is discussed further by Voss in Ref. 13. Figure 1(a) is the average of over sixty samples from the Pacific and Atlantic Oceans collected during 1983. The data points and standard deviations are given in Tables I–IV. These are ensemble standard deviations; they represent the variability over the entire sample set, not the error in the individual samples. For reference, the phase functions, normalized to unity at 90°, of some Atlantic and Pacific samples are shown in Fig. 2.

The most striking feature in all the measured matrices is the number of zero elements. The normalized matrix elements are much like those of particles in the Rayleigh-Gans or Rayleigh limit [shown in Fig. 1(b)], implying low index or very small particulates.

A consistent feature in all the measured matrices is the deviation of the S22 element from 1.0; it falls off to a broad minimum of between 0.6 and 0.8 at a scattering angle of ~100°. This element has been shown to deviate from 1.0 when measuring nonspherical particles.[15,16] Consequently, this deviation in ocean water is not surprising since oceanic hydrosols are generally nonspherical.

The matrix elements S12 and S21 are observed to be very similar and reach a minimum of between −0.6 and −0.8 at scattering angles near 90°. For comparison, in the Rayleigh approximation, S12 is equal to S21 and reaches −1.0 at 90° indicating full linear polarization at 90°. Although the normalized matrix elements observed for our ocean water samples tend to have the same shape as in Rayleigh scattering, this full polarization does not occur.

The last matrix elements which are nonzero are the S33 and S44 elements. These elements also look quite similar to the Rayleigh matrix elements in form; however they differ in two respects. In the backward direction (around a scattering angle of 160°) these matrix elements will reach a value of only from −0.70 to −0.85 rather than almost −1.0 as in the Rayleigh scattering approximation. In addition, these matrix elements are zero at scattering angles in the range of 90° and 95° rather than at precisely 90° as in the Rayleigh scattering case. For example, at 90°, S33 may have a nonzero value which is up to three or four times the normal systematic error limit.

As a specific example of this effect we present the data of Figs. 3(a) and (b) from samples located at the position 40° 08.46'N, 70° 56.65'W in the Atlantic Ocean. These are, respectively, the measured matrices from depths of 28 and 143 m at this position. The phase functions for these two samples were shown in Fig. 2, with $\beta(45)$ varying by 30% between the samples. The first example, Fig. 3(a), is a sample in which the S33 and S44 matrix elements cross above 90°; the second, Fig. 3(b), is a sample for which the S33 and S44 matrix elements cross at 90°. The latter sample is from a depth of 143 m, which was ~5 m from the bottom. This depth corresponded to a minimum in the reading of a transmissometer and a very low chlorophyll fluorescence reading. Hence the particulates consisted of mostly sediment or detrital material with a very low level of viable phytoplankton material. The former sample [Fig. 3(a)] was from a depth where there was a high chlorophyll fluorescence reading and a low transmittance implying a comparatively high level of viable phytoplankton. We emphasize that the effect, although small, is real. The Rayleigh scattering standard was examined before and after each measurement to verify proper operation of the instrument. Furthermore, the measurements were repeated three times and clearly showed the effect was reproducible.

Another point to be emphasized deals with the variability of the matrix elements between samples. Kadyshevich and Lyubovtseva[7] found that the greatest variability for S12 was at 25–35°, and for S33 and S44 the largest variability was at 25–45° and at angles around 145°. As can be seen from Tables I–IV, we found the greatest variability for S12 and S21 was around 90°, and for S22 it was around 100°. For S33 and S44 the region of largest variability was spread from 60° to 160°. Comparatively little variability was observed in all matrix elements at 25–35°.

V. Error Analysis

For this instrument the dominant error is systematic and is due to misalignment of the optical components of the system (modulators, polarizers, position of the sample cell). Of these the most important error is due to the misalignment of the modulators and has been discussed in detail by Bottiger[17] and Thompson.[11] When misalignment occurs it causes mixing in neighboring matrix elements. This mixing has the most pronounced effect on matrix elements which are small,

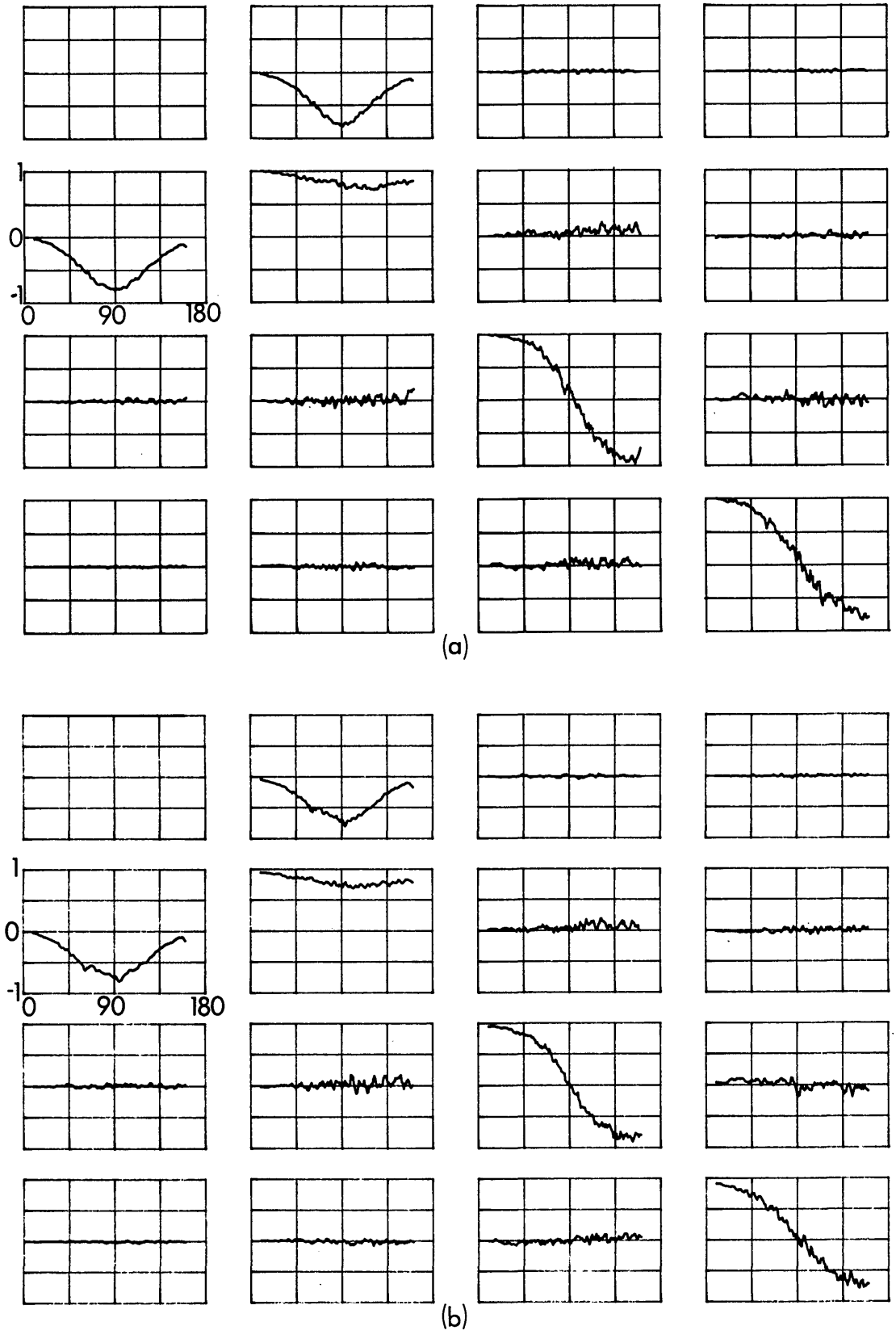

Fig. 3. Samples from the Atlantic Ocean at a position 40° 08.46′N, 70° 56.68′W: (a) 28-m depth, (b) 143-m depth.

Table I. Mean Data Points and Standard Deviations of the Mueller Matrix for Ocean Water Samples from the Pacific and Atlantic Oceans, First Row

Angle	S12 Ave	Std	S13 Ave	Std	S14 Ave	Std
10	−0.03	0.01	0.00	0.01	0.00	0.01
15	−0.05	0.02	−0.00	0.01	−0.01	0.01
20	−0.06	0.02	−0.00	0.01	−0.01	0.01
25	−0.09	0.02	−0.01	0.01	−0.01	0.01
30	−0.12	0.02	−0.01	0.01	−0.01	0.01
35	−0.15	0.02	−0.01	0.01	−0.01	0.01
40	−0.19	0.02	−0.01	0.01	−0.01	0.01
45	−0.24	0.02	−0.01	0.01	−0.01	0.01
50	−0.29	0.03	−0.01	0.01	−0.01	0.01
55	−0.36	0.03	−0.01	0.01	−0.01	0.02
60	−0.42	0.05	−0.01	0.01	−0.01	0.01
65	−0.47	0.05	−0.01	0.01	−0.01	0.02
70	−0.53	0.05	−0.01	0.02	−0.01	0.02
75	−0.59	0.06	−0.01	0.02	−0.01	0.02
80	−0.62	0.07	−0.01	0.02	−0.01	0.02
85	−0.65	0.08	−0.01	0.02	−0.01	0.02
90	−0.66	0.09	−0.01	0.02	−0.01	0.02
95	−0.66	0.09	−0.01	0.02	−0.01	0.02
100	−0.63	0.09	−0.01	0.02	−0.01	0.02
105	−0.59	0.08	−0.01	0.03	−0.01	0.02
110	−0.54	0.08	−0.01	0.03	−0.01	0.02
115	−0.49	0.06	−0.02	0.03	−0.01	0.02
120	−0.43	0.05	−0.01	0.02	−0.01	0.02
125	−0.37	0.05	−0.01	0.02	−0.02	0.02
130	−0.30	0.04	−0.01	0.02	−0.01	0.02
135	−0.25	0.03	−0.01	0.02	−0.01	0.02
140	−0.21	0.02	−0.01	0.02	−0.01	0.01
145	−0.16	0.03	−0.01	0.02	−0.01	0.01
150	−0.14	0.02	−0.01	0.01	−0.01	0.02
155	−0.12	0.02	−0.01	0.01	−0.01	0.01
160	−0.12	0.03	−0.01	0.01	−0.01	0.01

Table II. Mean Data Points and Standard Deviations of the Mueller Matrix for Ocean Water Samples from the Pacific and Atlantic Oceans, Second Row

Angle	S21 Ave	Std	S22 Ave	Std	S23 Ave	Std	S24 Ave	Std
10	0.00	0.03	0.98	0.06	0.02	0.03	−0.04	0.03
15	−0.02	0.03	0.97	0.06	0.02	0.03	−0.04	0.03
20	−0.05	0.03	0.96	0.05	0.02	0.03	−0.04	0.03
25	−0.08	0.03	0.95	0.04	0.01	0.03	−0.04	0.03
30	−0.11	0.03	0.94	0.04	0.02	0.04	−0.04	0.02
35	−0.16	0.03	0.93	0.05	0.02	0.04	−0.04	0.03
40	−0.21	0.03	0.92	0.05	0.01	0.04	−0.04	0.03
45	−0.26	0.03	0.91	0.06	0.02	0.05	−0.03	0.03
50	−0.32	0.04	0.89	0.05	0.02	0.05	−0.03	0.03
55	−0.39	0.04	0.86	0.05	0.02	0.05	−0.03	0.04
60	−0.45	0.05	0.85	0.06	0.02	0.07	−0.02	0.04
65	−0.51	0.05	0.82	0.06	0.01	0.07	−0.02	0.04
70	−0.56	0.06	0.78	0.07	0.01	0.08	−0.02	0.04
75	−0.61	0.07	0.76	0.08	0.01	0.09	−0.02	0.04
80	−0.62	0.09	0.72	0.09	−0.00	0.07	−0.02	0.04
85	−0.65	0.09	0.70	0.10	0.00	0.09	−0.01	0.05
90	−0.66	0.10	0.69	0.10	0.00	0.10	−0.02	0.05
95	−0.66	0.09	0.68	0.10	0.10	0.11	−0.01	0.05
100	−0.63	0.09	0.68	0.10	−0.01	0.10	0.01	0.05
105	−0.59	0.09	0.67	0.10	0.00	0.10	−0.01	0.05
110	−0.54	0.08	0.66	0.10	0.00	0.10	0.00	0.05
115	−0.48	0.08	0.66	0.12	0.00	0.09	0.00	0.05
120	−0.42	0.07	0.67	0.11	0.00	0.11	0.00	0.05
125	−0.37	0.05	0.69	0.09	0.01	0.09	0.01	0.05
130	−0.31	0.04	0.71	0.09	0.01	0.08	0.02	0.05
135	−0.26	0.03	0.72	0.07	0.01	0.10	0.02	0.05
140	−0.21	0.03	0.74	0.06	0.01	0.09	0.02	0.05
145	−0.16	0.03	0.75	0.09	0.01	0.10	0.02	0.05
150	−0.13	0.03	0.76	0.08	0.01	0.10	0.01	0.04
155	−0.10	0.02	0.77	0.06	0.00	0.09	0.02	0.04
160	−0.10	0.05	0.78	0.06	−0.01	0.08	0.02	0.04

Table III. Mean Data Points and Standard Deviations of the Mueller Matrix for Ocean Water Samples from the Pacific and Atlantic Oceans, Third Row

Angle	S31 Ave	Std	S32 Ave	Std	S33 Ave	Std	S34 Ave	Std
10	0.00	0.01	0.04	0.03	0.97	0.08	0.01	0.05
15	0.00	0.01	0.04	0.03	0.96	0.08	−0.01	0.04
20	0.00	0.01	0.04	0.03	0.96	0.07	−0.01	0.05
25	−0.01	0.01	0.04	0.03	0.96	0.05	0.01	0.05
30	0.00	0.01	0.04	0.03	0.92	0.06	0.02	0.06
35	−0.01	0.01	0.04	0.04	0.91	0.06	0.03	0.06
40	0.00	0.01	0.04	0.03	0.89	0.06	0.02	0.06
45	0.00	0.01	0.04	0.04	0.85	0.07	0.03	0.06
50	−0.01	0.01	0.04	0.05	0.81	0.07	0.03	0.06
55	−0.01	0.02	0.03	0.06	0.76	0.07	0.01	0.06
60	−0.01	0.02	0.04	0.07	0.69	0.09	0.02	0.07
65	−0.01	0.02	0.04	0.07	0.61	0.09	0.01	0.07
70	0.00	0.02	0.05	0.06	0.52	0.10	0.01	0.07
75	0.00	0.02	0.04	0.10	0.42	0.10	0.00	0.07
80	0.00	0.02	0.05	0.10	0.30	0.11	0.01	0.07
85	0.00	0.02	0.04	0.09	0.18	0.09	0.00	0.07
90	0.01	0.03	0.05	0.10	0.07	0.08	−0.01	0.09
95	0.00	0.03	0.05	0.09	−0.06	0.09	−0.01	0.08
100	0.01	0.03	0.06	0.10	−0.18	0.09	−0.01	0.08
105	0.01	0.03	0.07	0.11	−0.27	0.10	0.01	0.09
110	0.01	0.03	0.06	0.10	−0.39	0.10	−0.01	0.09
115	0.01	0.03	0.05	0.10	−0.46	0.13	0.00	0.08
120	0.01	0.03	0.04	0.10	−0.53	0.13	−0.02	0.08
125	0.01	0.03	0.05	0.10	−0.61	0.12	0.00	0.08
130	0.01	0.03	0.04	0.10	−0.66	0.12	0.00	0.08
135	0.01	0.03	0.05	0.10	−0.70	0.12	0.00	0.08
140	0.01	0.03	0.05	0.09	−0.73	0.10	0.00	0.07
145	0.01	0.02	0.05	0.09	−0.75	0.12	0.00	0.08
150	0.01	0.02	0.05	0.08	−0.77	0.11	−0.01	0.08
155	0.01	0.02	0.06	0.08	−0.77	0.09	0.00	0.07
160	0.02	0.02	0.06	0.08	−0.74	0.09	−0.01	0.07

Table IV. Mean Data Points and Standard Deviations of the Mueller Matrix for Ocean Water Samples from the Pacific and Atlantic Oceans, Fourth Row

Angle	S41 Ave	Std	S42 Ave	Std	S43 Ave	Std	S44 Ave	Std
10	0.02	0.02	0.00	0.02	−0.02	0.05	0.97	0.08
15	0.02	0.02	0.00	0.02	−0.01	0.05	0.97	0.08
20	0.02	0.02	0.00	0.02	−0.01	0.05	0.97	0.07
25	0.03	0.02	0.02	0.03	−0.04	0.05	0.96	0.06
30	0.02	0.02	0.01	0.03	−0.05	0.06	0.92	0.06
35	0.02	0.02	0.01	0.03	−0.05	0.06	0.90	0.06
40	0.02	0.02	0.01	0.03	−0.04	0.06	0.88	0.06
45	0.02	0.02	0.00	0.04	−0.05	0.06	0.84	0.07
50	0.02	0.02	0.00	0.04	−0.04	0.07	0.79	0.07
55	0.03	0.03	0.00	0.04	−0.04	0.06	0.75	0.09
60	0.02	0.02	0.00	0.05	−0.04	0.06	0.67	0.10
65	0.02	0.03	0.00	0.06	−0.04	0.05	0.59	0.10
70	0.02	0.03	−0.02	0.05	−0.04	0.05	0.50	0.11
75	0.02	0.03	−0.01	0.08	−0.03	0.06	0.40	0.09
80	0.02	0.03	−0.01	0.06	−0.02	0.06	0.29	0.10
85	0.02	0.03	−0.02	0.08	−0.03	0.06	0.17	0.10
90	0.02	0.03	−0.02	0.08	−0.02	0.08	0.06	0.11
95	0.02	0.03	−0.02	0.07	−0.02	0.06	−0.05	0.10
100	0.02	0.03	−0.03	0.11	−0.01	0.07	−0.16	0.11
105	0.02	0.03	−0.03	0.10	−0.02	0.07	−0.24	0.12
110	0.02	0.03	−0.04	0.07	−0.01	0.07	−0.33	0.12
115	0.02	0.03	−0.03	0.09	−0.01	0.06	−0.39	0.11
120	0.02	0.03	−0.04	0.09	−0.02	0.07	−0.48	0.10
125	0.02	0.03	−0.03	0.08	−0.01	0.06	−0.54	0.12
130	0.02	0.03	−0.04	0.08	−0.02	0.07	−0.60	0.11
135	0.03	0.03	−0.05	0.08	−0.02	0.06	−0.63	0.12
140	0.02	0.03	−0.04	0.07	−0.01	0.06	−0.66	0.10
145	0.02	0.02	−0.04	0.08	0.00	0.06	−0.69	0.11
150	0.03	0.03	−0.05	0.08	0.00	0.06	−0.72	0.11
155	0.03	0.02	−0.05	0.07	0.00	0.05	−0.71	0.08
160	0.02	0.02	−0.02	0.07	0.01	0.05	−0.68	0.09

or zero, and which occupy positions in the matrix adjacent to large nonzero elements. In the case of seawater, S23, S32, S34, and S43 are most likely to show noticeable alignment error. Mixing in these matrix elements is very difficult to reduce below 2% of full scale, but with care in alignment, the mixing in all other matrix elements can be reduced to below 0.5%. In normal operation at sea these errors can be somewhat larger, up to 5–10% and 1–5%, respectively. The accuracy of the matrix is determined by measuring Rayleigh sphere standards (0.091-μm polystyrene spheres in water) and comparing the measured matrix of these spheres with the theoretical Rayleigh matrix.

A second source of systematic error arises from drifts in the photomultiplier tube dark current. This dark current is carefully measured and an analog signal which reproduces it is stored in the instrument; analog techniques are then used to subtract it from the photomultiplier tube signal in order to obtain the true dc component of the signal.[13] The latter is used to normalize the matrix and hence drifts in the dark current will produce systematic errors in the entire matrix. The effect is most pronounced at signal levels comparable to the dark current. It is suppressed to negligible levels by temperature stabilization of the photomultiplier tube with a circulating constant temperature bath. In addition, signal levels are always checked to verify that they are greater than approximately four times the dark current signal.

Finally, there is an important systematic effect due to drifts in the electronics. This can easily produce 1–2% shifts in the zero of a matrix element or in its full scale value. This problem is handled by simply checking the zero levels and the full scale amplitudes frequently.

There are three main noise sources—laser amplitude noise, photomultiplier tube noise, and noise due to fluctuations in the observed sample volume. Laser amplitude noise at the reference frequencies for the various matrix elements produces white noise at the lock-in outputs of the respective matrix elements. Furthermore, any ripple frequency in the laser intensity (for example, a 60-Hz ripple) produces sidebands in the detected intensity; these can lie very close to a reference frequency and produce slow, small oscillations in the respective lock-in output. A laser intensity regulator can be used to effectively eliminate laser amplitude noise,[18] however, this device was not used for most of the data presented here.

Even if the laser intensity is noiseless, the detection process is statistical and the signal from the photomultiplier tube will fluctuate. In particular, the signal current at the anode is given by

$$i_s = \mathrm{AneN}, \tag{5}$$

where N is the number of photons incident on the cathode per unit time, e is the electron charge, n is the photocathode quantum efficiency, and A is the gain of the dynode stack. Similarly, the noise current in a bandwidth B is

$$i_n = A\sqrt{2e^2n(l-n)NB}, \tag{6}$$

where for simplicity we have assumed the incident photon flux is noiseless. Now in our instrument the matrix is normalized by keeping the signal current constant. Specifically, as N changes, a feedback circuit adjusts the gain A so that

$$NA = K, \tag{7}$$

where K is a constant. In these conditions the anode noise current is

$$i_n = \sqrt{2Ae^2n(l-n)BK}. \tag{8}$$

Thus i_n is proportional to $\sqrt{A}$ and is a maximum when A is maximum or equivalently when the incident photon flux is a minimum. For ocean water N is a minimum at scattering angles between 90° and 135° and the increased noise in this angular range is readily apparent in Fig. 2.

Finally, there is noise due to particles drifting in or out of the observed scattering volume. Small particles generally occur in sufficient numbers that noise due to their statistical fluctuations is significantly smaller than that of the other sources. However, when a large (>100-μm) particle drifts through the sample volume it causes an obvious nonreproducible fluctuation in the matrix elements. These large particles are not common in our measurements.

The noise actually observed varies among matrix elements mainly for the following reason. Each Fourier coefficient corresponding to a matrix element is the multiple of the matrix element and one to four Bessel functions, of order 1 or 2, evaluated at 137°. Therefore to normalize the matrix elements they have to be amplified by different factors to adjust for these Bessel function products. The proportionality factors with respect to the S12 element are

$$\begin{array}{cccc} & 1 & 1.59 & 1.92 \\ 1 & 2.32 & 3.70 & 4.46 \\ 1.59 & 3.70 & 5.88 & 7.09 \\ 1.92 & 4.46 & 7.09 & 8.62 \end{array}. \tag{9}$$

For example, the S44 element has to be amplified 8.62 times more than the S12 element. Therefore, assuming all other factors are constant (i.e., white noise and identical amplifier bandwidths), the noise in S44 is a factor of 8.62 larger than the noise in S12. The observed noise also differs between matrix elements due to the wide range of audio frequencies over which the matrix elements are measured (0.9–20 kHz) and to various observation bandwidths. However, the above effect can be seen in the data of Fig. 2, particularly in the relatively low noise amplitudes for S13, S14, S31, and S41. In practice all noise effects are reduced by making at least three measurements of a sample and averaging them.

In summary, some matrix elements have overall errors typically <2% (S12, S13, S14, S21, S31, and S41), and some matric elements <5% (S22, S33, and S44). The accuracy of matrix elements S23, S32, S34, and S43 is strongly dependent on the angle, yaw, and pitch of EOMs 2 and 3. It is often difficult to maintain their

Table V. Mean Data Points and Standard Deviations of the S32 Element for Rayleigh Standards

Angle	S32 Ave	Std
10	0.04	0.03
15	0.04	0.03
20	0.03	0.04
25	0.03	0.03
30	0.04	0.04
35	0.04	0.04
40	0.04	0.03
45	0.04	0.06
50	0.05	0.05
55	0.03	0.05
60	0.05	0.06
65	0.05	0.04
70	0.04	0.06
75	0.06	0.08
80	0.04	0.05
85	0.04	0.07
90	0.05	0.09
95	0.03	0.06
100	0.04	0.07
105	0.06	0.06
110	0.02	0.06
115	0.04	0.06
120	0.03	0.07
125	0.00	0.05
130	0.02	0.05
135	0.02	0.07
140	0.02	0.05
145	0.03	0.08
150	0.02	0.06
155	0.03	0.04
160	0.04	0.05

alignment accurately, particularly at sea. Consequently, the error in these matrix elements sometimes reaches 10%.

As with any measurement system, the use of an absolute standard whose properties are close to those being measured can considerably increase the level of confidence in the results. For this work the standard was the dilute aqueous suspension of 91-nm diam polystyrene spheres; this system is a Rayleigh scatterer for visible light. It was customary to regularly check the instrument operation by measuring this standard. However, to avoid any ambiguities associated with modifying data, the results presented in this paper were never adjusted for mixing effects (systematic errors) indicated by this Rayleigh data. Rather, Rayleigh data were used mainly to tune the instrument and thereby minimize mixing effects in subsequent data sets.

However, the Rayleigh data do provide additional and important insight into the ocean measurements. For example, the large nonzero matrix elements adjacent to elements S23, S32, S34, and S43 can, through alignment errors, mix into these elements and cause them to appear to be nonzero. If this occurred for an ocean sample, the associated Rayleigh calibrations generally exhibited the same nonzero values indicating that the effect was systematic. Such systematic errors typically averaged to zero but resulted in relatively large standard deviation for these four matrix elements, as can be seen in Tables II–IV. Consequently the standard deviations for these elements really represent variability in the systematics for these elements rather than sample variability. On the other hand the elements S12, S21, S22, S33, and S44 for ocean water do not have large adjacent nonzero elements which can easily mix into them. This is borne out by the measurements of the Rayleigh standard. The standard deviations for these elements are definitely due to sample variability.

As a specific example, consider S32 which had the largest systematics in the ocean data. The ensemble averaged Rayleigh data for this element are given in Table V. The agreement with the corresponding data in Table III is very good. Consequently, setting S32 = 0.0 in the representative ocean water matrix is clearly justified. Identical arguments hold for the other null matrix elements.

VI. Numerical Comparisons

Ocean water Mueller matrices cannot be precisely modeled because of the large variety of hydrosol shapes and sizes and because only a small number of particle shapes (spheres, infinite cylinders, ellipses) can be calculated; therefore, approximations must be made to do the calculations. It has been argued[16,19] that reasonable fits to the phase function (matrix element M11) of asymmetric particles can be obtained for scattering angles from 0° to 80° using spheres. This has encouraged investigators[20,21] to approximate the particles in the ocean as spheres and use Mie codes to model the phase function of ocean water measurements by appropriate choices of size distributions.

Several such distributions have been developed and we have used them to calculate Mueller matrix elements with a Mie code computer program supplied by G. W. Kattawar. This code calculated the Mueller matrix elements of spheres of a given size distribution and index of refraction. The results were compared to the experimentally observed matrices of ocean water samples.

The first distribution studied was that of Gordon and Brown.[22] This was a one-component distribution with index of refraction $1.05–0.01i$ and size distribution $dN/dD = K/D^4$, where D is the diameter of the particles and K is a constant chosen to give the correct overall number of particles as given by Coulter counter measurements of Sargasso Sea water. The size range used was D values from 0.08 to 10 μm. The results of this calculation are shown in Fig. 4. The polarization data are very close to the Rayleigh approximation. The obvious features are that the S33 element is zero at an angle of 93°, and the S43 elements stays at very low values (<0.02) at all angles. The major differences between these calculations and measured ocean water samples are the magnitudes of the minimum S12 value, the S33 value in the backward direction, and the value of the S22 matrix element (which is unity at all scattering angles in any Mie calculation regardless of the size distribution). Here a comment is in order.

By examining the Mueller matrix elements, Fry and Kattawar[23] derived a series of relationships which must hold for a Mueller matrix of a collection of particles.

For one particle in a single orientation the relationships were equalities, but for more than one particle, or particles in random orientation, these relationships become inequalities. Some general restrictions applicable to the ocean water data can be derived using these inequalities.

In the measurements of ocean water the general form of the matrix has been found to be

$$\begin{bmatrix} 1 & -d & 0 & 0 \\ -e & 1-a & 0 & 0 \\ 0 & 0 & b & f \\ 0 & 0 & -g & c \end{bmatrix}, \tag{10}$$

In most of our measurements (g) and (f) have been zero to the accuracy of our instrument. Also (b) and (c) as well as (e) and (d) have been almost identical. Therefore, in these calculations we will assume that $g = f = 0$, $b = c$, and $e = d$ to simplify analysis.

Equation (10c) in the paper by Fry and Kattawar[23] states that

$$(M11 + M21)^2 - (M12 + M22)^2 > (M13 + M23)^2 + (M14 + M24)^2. \tag{11}$$

Applied to the above matrix this equation becomes

$$d < 1 - a/2. \tag{12}$$

This restriction shows that, since $a > 0$, then $|d|$ cannot be unity but must be less by at least $a/2$.

By Eq. (10a) in the same paper by Fry and Kattawar[23] it can be shown that

$$d^2 + c^2 < (1 - a/2)^2. \tag{13}$$

This equation is even more restrictive than Eq. (12) and, in fact, reduces to Eq. (12) when $c = 0$.

Now a, the deviation of S22 from 1.0, has been shown to occur with nonspherical particles and also in our ocean measurements. The above restrictions show that, since a is not equal to 0, then $|d|$ cannot be 1 but must be less by at least $a/2$. Since any calculations using Mie theory will give $a = 0$ (or equivalently S22 = 1) at all angles and for all sizes, they cannot reproduce either the S22 for ocean water or any of the effects in other matrix elements required by its deviation from unity. To clarify these effects, the above restrictions were used to modify the calculations shown in Fig. 4 by assuming S22 values corresponding to those measured for ocean water samples.

The results for the matrix is shown in Fig. 5. For this heuristic study the values for S33 and S12 (i.e., c and d) were squared then summed. If the number resulting

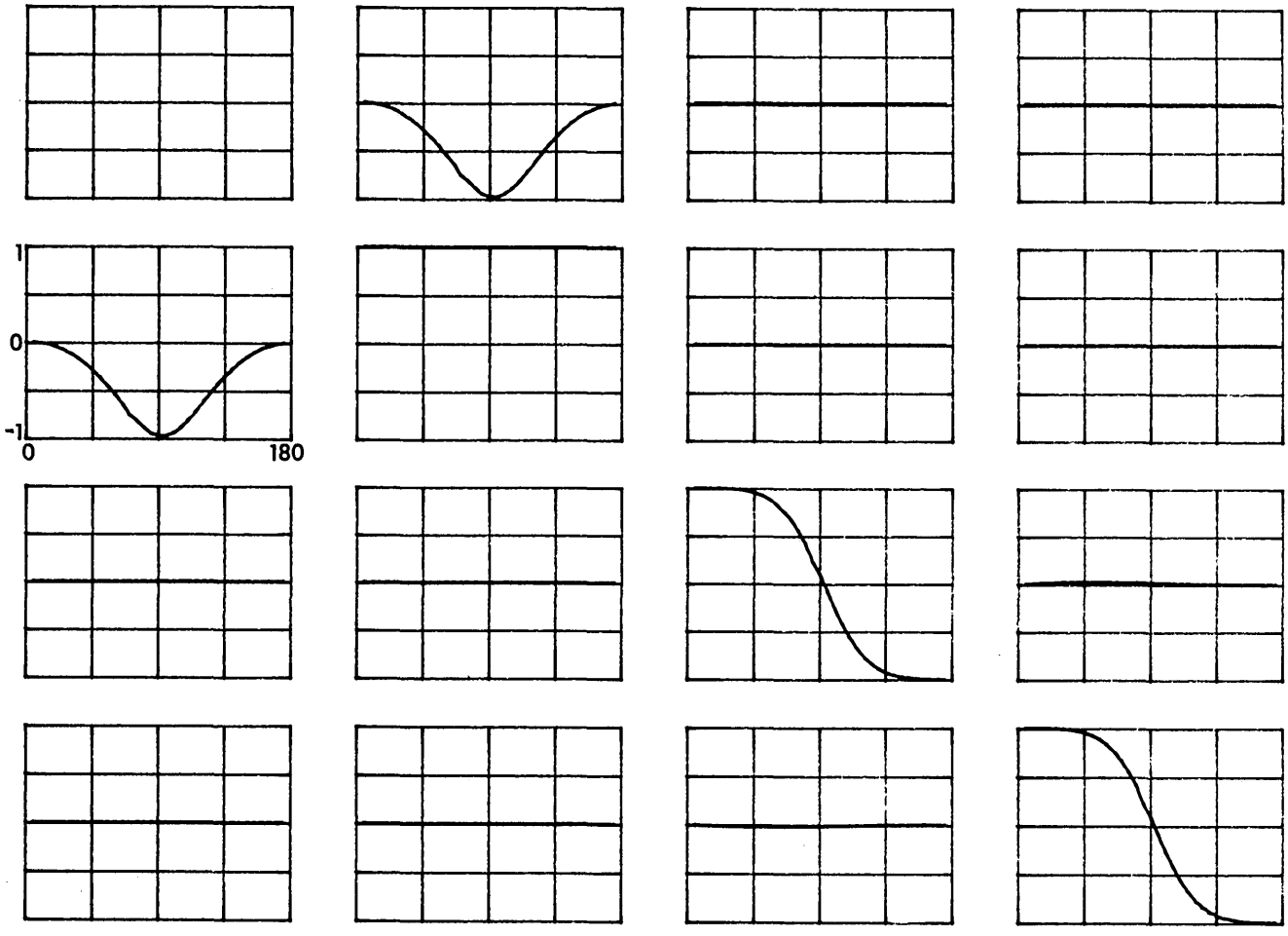

Fig. 4. Mueller matrix of calculation with index of refraction 1.05–0.01i and size distribution $dN/dD = K/D^4$.

was larger than that required by the measured S22 and the above restriction [Eq. (13)], S33 and S12 were multiplied by a common factor which would reduce them as required. This resultant matrix provides a fairly good fit to the measured ocean water matrix elements which are shown by the dashed lines in Fig. 5.

Other distributions studied were by Brown and Gordon[21] and Zaneveld *et al.*[20] These distributions produced phase functions which corresponded to the Sargasso Sea phase functions by Kullenberg.[24] The phase function fit was better than the simple one-component distribution of Gordon and Brown,[22] but the Mueller matrices differed significantly from the measured matrices. For example, the representative matrix elements obtained from the Zaneveld *et al.*[20] distribution are shown in Fig. 6.

Due to the large number of elements in the off-diagonal quadrants which were measured to be zero, a calculation was done to estimate the magnitude expected for these elements due to the optical activity of chlorophyll *a* in phytoplankton. Shown in Fig. 7 is the upper right quadrant of the calculated matrix for *Platymonas suecica*. Values for the circular dichroism and optical rotation of chlorophyll *a* were obtained from Houssier and Sauer.[25] The value for the concentration of chlorophyll in *Platymonas suecica* was obtained from Morel and Bricaud.[26] The chlorophyll was assumed to be homogeneous in the cell and the cells were assumed to be within the Rayleigh-Gans limit. These results should provide an estimate of the size of these effects. As can be seen from Fig. 6, the measurements must be accurate to one part in 10^4 for these effects to be observed.

VII. Conclusion

The most important conclusion of this study is that the Mueller matrix for ocean water has in general one form. To within experimental error all off-diagonal elements other than S12 and S21 are zero, indicating little effect due to optical activity or orientational anistropy. This is important for those involved in radiation transfer; one form of the matrix can be used in these calculations to a relatively high degree of accuracy. If one were to use results from Tables I–IV in a radiation transfer calculation, all off-diagonal elements except S12 and S21 can be set to zero. Also, it is appropriate within the ensemble standard deviations to define an average $\overline{S12} = \overline{S21}$ to be the average of the measured S12 and S21 and to define an average $\overline{S33} = \overline{S44}$ to be

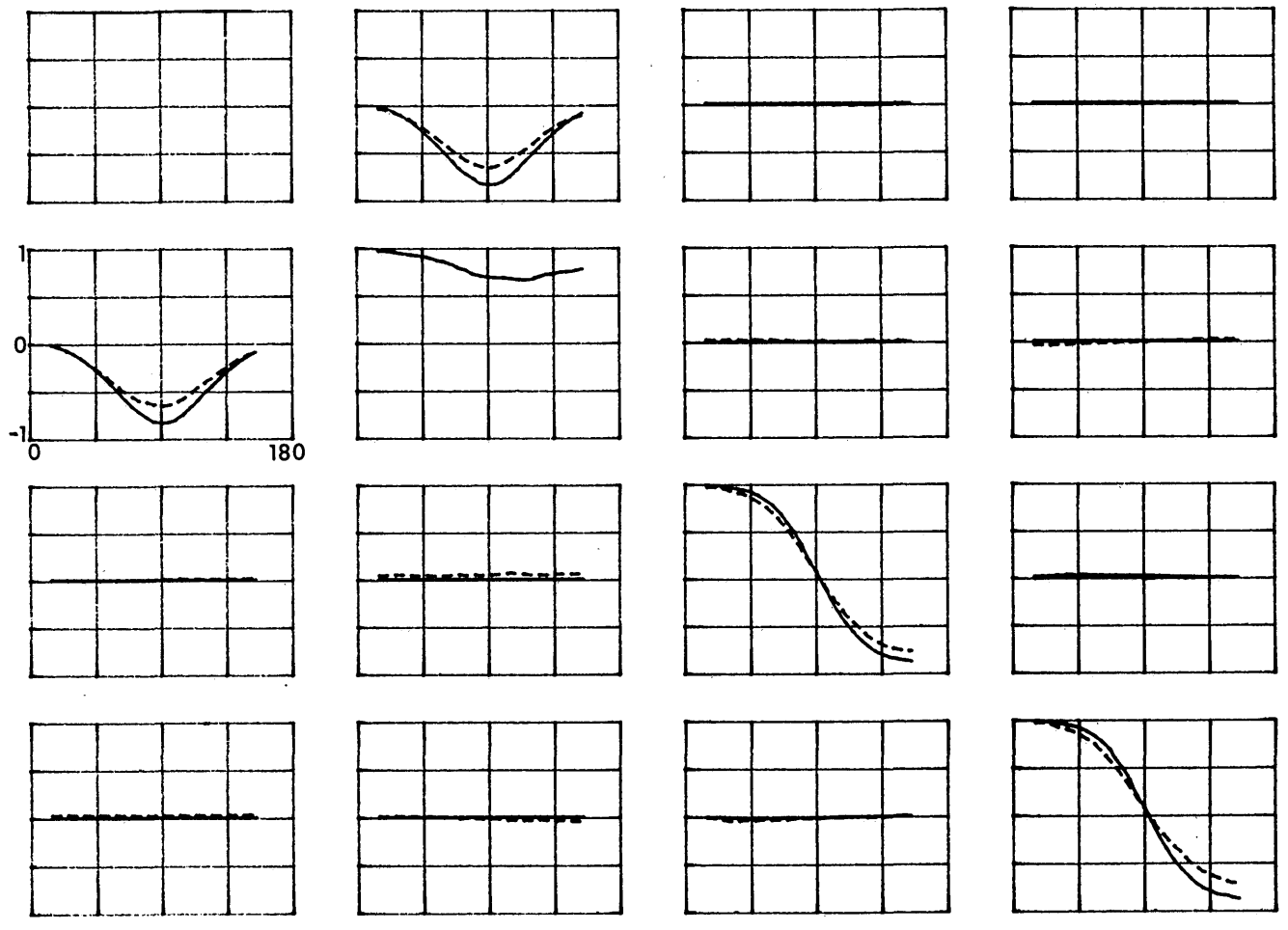

Fig. 5. Solid line, Mueller matrix elements of Fig. 4 modified to conform with S22 for ocean water; dashed line, ocean water data of Fig. 1(a).

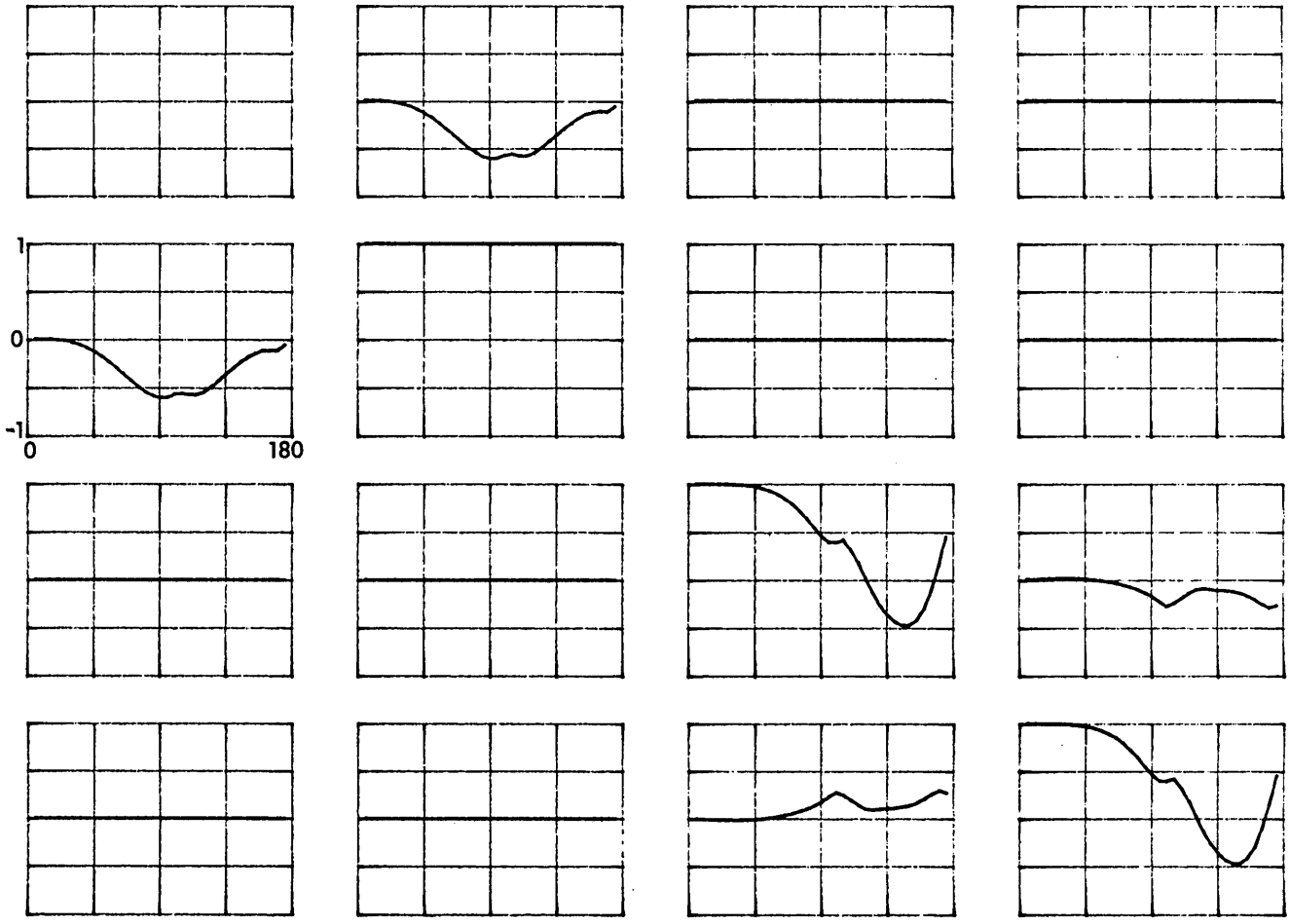

Fig. 6. Mueller matrix of calculation with index of refraction and size distribution after Zaneveld *et al.*[20]

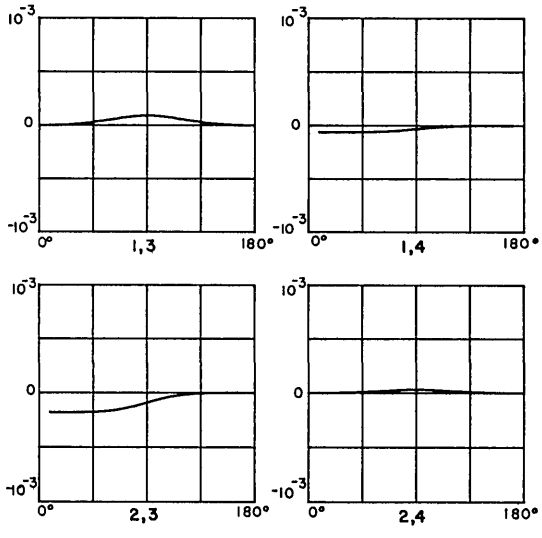

Fig. 7. Calculation of Mueller matrix elements for *Platymonas suecica*.

the average of the measured S33 and S44. In this event the normalized matrix is described by three angular dependent functions, S12, S22, and S33. This description represents an ocean matrix with a maximum standard deviation at any data point of 13%; in fact 95% of the data points have a standard deviation of 10% or less. The three functions and the associated standard deviations are given in Table VI.

In computer fits to the phase function many variations of parameters can be used to fit the same phase function. However, most of these will not reproduce all the measured scattering effects. In fact, one will never be able to model the ocean particulates with a Mie code exactly (as seen from our S22 element).

At the level of accuracy of this instrument one gains some information on the particulates in the ocean. For example, samples which have either phytoplankton or inorganic particulates appear to be distinguishable via the zero to S33. However to get really useful information, measurements are needed at a much higher level of accuracy. At a level of accuracy corresponding to one part of 10^4 one would probably see effects due to anisotropy either in shape, orientation, or optical activity.

Table VI. Average Nonzero Matrix Elements and Standard Deviations for the Ensemble of Samples

	$\overline{S12} = \overline{S21}$		S22		$\overline{S33} = \overline{S44}$	
Angle	Ave	Std	Ave	Std	Ave	Std
10	−0.02	0.03	0.98	0.05	0.97	0.07
15	−0.03	0.03	0.97	0.06	0.97	0.08
20	−0.05	0.03	0.96	0.05	0.96	0.07
25	−0.08	0.03	0.95	0.04	0.96	0.06
30	−0.11	0.03	0.94	0.04	0.92	0.06
35	−0.16	0.03	0.93	0.05	0.90	0.06
40	−0.20	0.03	0.92	0.05	0.89	0.06
45	−0.25	0.03	0.91	0.06	0.84	0.07
50	−0.31	0.04	0.89	0.05	0.80	0.08
55	−0.37	0.04	0.86	0.05	0.75	0.08
60	−0.43	0.05	0.85	0.06	0.68	0.09
65	−0.49	0.05	0.82	0.06	0.60	0.10
70	−0.55	0.06	0.78	0.07	0.51	0.10
75	−0.60	0.07	0.76	0.08	0.41	0.09
80	−0.62	0.08	0.72	0.10	0.30	0.10
85	−0.65	0.09	0.70	0.10	0.18	0.09
90	−0.66	0.10	0.69	0.11	0.07	0.10
95	−0.66	0.09	0.68	0.10	−0.05	0.09
100	−0.63	0.09	0.68	0.10	−0.17	0.10
105	−0.59	0.09	0.67	0.10	−0.26	0.11
110	−0.54	0.08	0.66	0.11	−0.36	0.11
115	−0.48	0.07	0.66	0.12	−0.43	0.13
120	−0.43	0.06	0.67	0.11	−0.51	0.12
125	−0.37	0.05	0.69	0.09	−0.58	0.12
130	−0.31	0.04	0.71	0.09	−0.63	0.12
135	−0.26	0.03	0.72	0.07	−0.67	0.13
140	−0.21	0.03	0.74	0.06	−0.70	0.11
145	−0.16	0.03	0.75	0.09	−0.72	0.12
150	−0.13	0.03	0.76	0.08	−0.75	0.11
155	−0.11	0.03	0.77	0.06	−0.74	0.09

References

1. N. G. Jerlov, "Ocean Light Scattering Properties Related to Dynamic Conditions," SPIE J. **8,** 89 (1970).
2. B. J. Price, V. H. Kollman, and G. C. Salzman, "Light-Scatter Analysis of Microalgae," Biophys. J. **22,** 29 (1978).
3. R. Spinrad, "Optical Characteristics and Physiological State of Marine Phytoplankton," AGU Ocean Sciences Meeting, 23–27 Jan. 1984, New Orleans, La.
4. R. Reeves, Ed., *Manual of Remote Sensing Vol. 2* (American Society of Photogrammetry, Va., 1975), p. 1573.
5. G. F. Beardsley, Jr., "Mueller Scattering Matrix of Sea Water," J. Opt. Soc. Am. **58,** 52 (1968).
6. Y. A. Kadyshevich, Y. S. Lyubovtseva, and I. N. Plakhina, "Measurement of Matrices for Light Scattered by Sea Water," Izv. Acad. Sci. USSR Atmos. Oceanic Phys. **7,** 557 (1971).
7. Y. A. Kadyshevich and Y. S. Lyubovtseva, and G. V. Rozenberg, "Light-Scattering Matrices of Pacific and Atlantic Ocean Waters," Izv. Acad. Sci. USSR Atmos. Oceanic Phys. **12,** 106 (1976).
8. Y. A. Kadyshevich, "Light-Scattering Matrices of Inshore Waters of the Baltic Sea," Izv. Acad. Sci. USSR Atmos. Oceanic Phys. **13,** 77 (1977).
9. H. C. van de Hulst, *Light Scattering By Small Particles* (Dover, New York, 1981).
10. G. G. Stokes, "On the Composition and Resolution of Streams of Polarized Light from Different Sources," Trans. Cambridge Philos. Soc. **9,** 399 (1853).
11. R. C. Thompson, "An Electro-Optic Light Scattering Photometric Polarimeter," Ph.D. Thesis, Texas A&M University (1978).
12. R. C. Thompson, J. R. Bottiger, and E. S. Fry, "Measurement of Polarized Light Interactions Via the Mueller Matrix," Appl. Opt. **19,** 1323 (1980).
13. K. J. Voss, "Measurement of the Mueller Matrix for Ocean Water," Ph.D. Thesis, Texas A&M University (1984).
14. N. G. Jerlov, *Marine Optics* (Elsevier, New York, 1976).
15. J. R. Bottiger, E. S. Fry, and R. C. Thompson, in *Light Scattering by Irregularly Shaped Particles*, D. W. Schuerman, Ed. (Plenum, New York, 1974), p. 283.
16. A. C. Holland and G. Gagne, "The Scattering of Polarized Light by Polydisperse Systems of Irregular Particles," Appl. Opt. **9,** 1113 (1970).
17. J. R. Bottiger, "Measured Light Scattering Matrices of Single Cubic Particles," Ph.D. Thesis, Texas A&M University (1978).
18. E. S. Fry, "Laser Intensity Regulator," J. Opt. Soc. Am. **66,** 1124 (1976).
19. G. N. Plass and G. W. Kattawar, "Comment on: The Scattering of Polarized Light by Polydisperse Systems of Irregular Particles. Part 1," Appl. Opt. **10,** 1172 (1971).
20. J. R. V. Zaneveld, D. M. Roach, and H. Pak, "The Determination of the Index of Refraction Distribution of Oceanic Particulates," J. Geophys. Res. **79,** 4091 (1974).
21. O. B. Brown and H. R. Gordon, "Two Component Mie Scattering Models of Sargasso Sea Particles," Appl. Opt. **12,** 2461 (1973).
22. H. R. Gordon and O. B. Brown, "A Theoretical Model of Light Scattering by Sargasso Sea Particulates," Limnol. Oceanogr. **17,** 826 (1972).
23. E. S. Fry and G. W. Kattawar, "Relationships Between Elements of the Stokes Matrix," Appl. Opt. **20,** 2811 (1981).
24. G. Kullenberg, "Scattering of Light by Sargasso Sea Water," Deep Sea Res. **15,** 423 (1968).
25. C. Houssier and K. Sauer, "Circular Dichroism and Magnetic Circular Dichroism of the Chlorophyll and Protochlorophyll Pigments," Amer. J. Chem. Soc. **92,** 779 (1970).
26. A. Morel and A. Bricaud, "Theoretical Results Concerning Light Absorption in a Discrete Medium, and Application to Specific Absorption of Phytoplankton," Deep Sea Res. **28A,** 1375 (1981).

This investigation has been supported by the Office of Naval Research through contract N00014-80-C-0113 and by the Texas A&M University Center for Energy and Mineral Resources contract 18789.